arXiv:cond-mat/0612587v1 [cond-mat.str-el] 22 Dec 2006

March 2006

Clear Experimental Signature of Charge-Orbital density wave in $Nd_{1-x}Ca_{1+x}MnO_4$:Heat Capacity and Magnetization study

Sher Alam[1], A.T.M.N. Islam[2], T.Nagai[1], M. Xu[1], Javed Ahmad[3], Y. Matsui[1], and I. Tanaka[2]

[1]*AML, NIMS, Tsukuba 305-0044, Ibaraki, Japan*

[2]*Crystal Group, Yamanashi University, Yamanashi, Japan*

[3]*Dept. of Physics, Bahauddin Zakariya University, Multan, Pakistan*

Abstract

Single Crystals of $Nd_{1-x}Ca_{1+x}MnO_4$ have been prepared by the traveling floating-zone method, and possible evidence of a charge -orbital density wave in this material presented earlier [PRB68,092405 (2003)] using High Resolution Electron Microscopy [HRTEM] and Electron Diffraction [ED]. In the current note we present direct evidence of charge-orbital ordering in this material using heat capacity measurements. Our heat capacity measurements indicate a clear transition consistent with prior observation. We find two main transitions, one at temperature $T_H^{HC} = 310-314$ K, and other in the vicinity of $T_A^{HC} = 143$ K. In addition, we may also conclude that there is a strong electron-phonon coupling in this material. In order to further study and confirm these anomalies we have performed dc magnetization measurements. The dc magnetic measurements confirm these two transitions. Again,we find two main transitions, one at temperature $T_H^M = 318 - 323$ K, and other at around $T_A^M = 164$ K.

PACS numbers: 78.20.-e, 78.30.-j, 74.76.Bz

1 Introduction

The transition-metal oxides display a wide variety of interesting properties. In particular of interest are the 3d transition metals such as Fe, Cu, Ni, Co and Mn, having a single layered perovskite structure, i.e. K_2NiF_4-type. These materials provide us useful insights into the underlying Mott-Hubbard in addition to helping us understand the superconducting oxides to which they are similar. In a recent note we [1] have shown the existence of inhomogenous charge distribution in very good quality single crystal of $LaSrCuO_4$ [LSCO] co-doped with 1% Zn at the copper site, using temperature dependent polarized X-ray absorption near-edge structure [XANES] spectra. A related single-layered compound to the LSCO is $LaSrFeO_4$ whose atomic and magnetic structure was first elucidated by Souberoux et al.[2], using X-ray diffraction, Mossbauer spectroscopy and neutron diffraction in polycrystalline state. Recently Kawanaka [3] have prepared a single crystal of $LaSrFeO_4$ by floating-zone method and demonstrated a spin flop transition in the antiferromagnetic ground state.

In particular it seems that 3d-electron systems exhibit ordering and disordering of the fundamental degrees of freedom such as charge, spin and orbital. In turn it is plausible that this may be responsible for metal-insulator transition[3], high-T_c superconductivity [1, 4], and colossal magnetoresistance [5]. A class of materials which show charge-orbital ordering of e_g electrons are the mixed valent manganites, the perovskite-type: $RE_{1-x}AE_xMnO_3$, single-layered $RE_{1-x}AE_{1+x}MnO_4$ and double-layered $RE_{2-2x}AE_{1+2x}Mn_2O_7$, where RE=trivalent lanthanides, and AE=divalent alkaline-earth ions. The real-space ordering pattern, possibly induced by strong electron-phonon interaction, that is a cooperative Jahn-Teller effect, can be determined by crystallographic superstructure [6, 7]. What physical insight can be gained from these crystallographic superstructure? Here are some examples, for the case of the over-doped single-layered manganites, the suggested models[7, 8] indicate that the Mn valence is not an integer but suffers a modulation from site to site. In addition two other theoretical proposals of some interest for the over-doped single-layered manganites, are the Wigner-crystal[9] and bi-stripe models[10]. The Wigner-crystal model [9] asserts the stacking of Mn^{3+} and Mn^{4+} stripes, such that Mn^{3+} stripes are regularly spaced, in contrast the bi-stripe model [10] claims the pairing of the Mn^{3+} stripes.

Thus main the purpose of this note is to concentrate on the experimental results of our heat capacity measurements for the layered manganites $Nd_{1-x}Ca_{1+x}MnO_4$. Previously two of us reported [6], using HRTEM and ED presence of super-reflections and transverse and sinusoidal modulations in the charge-orbital ordered phases. The previous measurements [6] were carried out using polycrystalline samples of $Nd_{1-x}Ca_{1+x}MnO_4$. Here we report for the first time the successful growth of single crystals of $Nd_{1-x}Ca_{1+x}MnO_4$ for x=0.67 and x=0.70. The Heat Capacity [HC] was measured using Quantum Design Physical Property Measurement System [PPMS].

The dc magnetization, was measured using Quantum Design SQUID magnetometer [MPMS].

This paper is organized as follows, in the next section we outline experimental details.

This is followed by section three where the results and discussion of our study are given. The final section contains the conclusions.

2 Experimental

It should be noted that we have for the first time succeeded in growing single crystals of $Nd_{1-x}Ca_{1+x}MnO_4$ for x=0.67 and x=0.70. It is non-trivial to do so, in particular for the case of high calcium content, i.e. $x \geq 0.72$ it was not possible to obtain single crystals.

The crystal growth was carried out using the floating zone technique in a four-mirror type infrared image furnace. Feed rod was prepared by solid state reactions: high purity powders of Nd_2O_3, $CaCO_3$ and MnO_2 were mixed in stoichiometric composition and were calcined twice at 1000 ^{o}C for 12 hours with intermediate grinding. In fact about 3% extra MnO_2 was mixed to compensate for the vaporization. The powder was then packed in a rubber tube and cold pressed under 300 MPa of pressure to a dense rod of 6 mm in diameter and 50-70 mm in length. The feed rod was then sintered at 1500 ^{o}C for 12 hours. Crystal growth was performed under flowing oxygen atmosphere at a speed of 5-10 mm/h.

To show the quality of the single crystal we have taken Laue x-ray diffraction pictures on the cleaved surface of the NCMO single crystals. Fig. 1 is given as an illustrative example, it can be clearly observed from this figure that there are clear spots and the expected four-fold symmetry in the (001) plane. We recall that the Space Group [SG] of NCMO-214 system is Bmab [SG number 64] above 220 K [roughly] and is Pccn [SG number 52] below 220 K, for both x=0.67 and x=0.70. For the composition x=0.60 below 160 K (roughly) SG of the fundamental structure: Pccn (56) and above 160K (roughly) SG of the fundamental structure: Bmab (64)

The HC of the sample is calculated by subtracting the addenda measurement from the total heat capcity measurement. The total HC is the measurement of the HC of the sample, the grease, and the sample platform. The two measurements-one with and one without the sample on the sample platform are necessary for accuracy. In order to ensure the further accuracy of our results, we conducted the experiment several times, each time repeating the addenda measurement. In addition, our several independent measurements are separated by 20-30 days.We note that automatic subtraction of the addenda, at each sample temperature measurement is performed. As we were interested mainly in the high temperature region, we used H-grease.

The dc magnetization measurements were performed with a SQUID magnetometer (MPMSXL, Quantum Design). Zero-field cooling (ZFC) measurements were carried out in the following way: first at zero field cooling down temperature from 390 to 5 K, then applying a field of 10000 Oe, and finally measuring the sample from 5 to 390 K in the field. Field cooling (FC) measurements were performed immediately after ZFC measurement from 390 to 5 K under 10000 Oe.

3 Results and Discussion

Figs. 2-5 show the results of HC measurements for the x=0.67 sample. Similarly the results are displayed in Figs. 6-9 when the composition is x=0.70. Let us call these cases I and II respectively. We note that both data are self-consistent, after one takes into account the simple factor due to the mass of the sample. The mass of the sample in case I was measured to be 5.25 $\pm$ 0.10 mg, and in case II 8.34 $\pm$ 0.10 mg. The clarity of the measurement is vividly displayed in Figs. 4 and 8. We can identify two main deviations from the normal at temperatures $T_{_H}$ and $T_{_A}$ in Figs. 3 and 7. The magnitude of the peaks is 5-15 % above the 'normal' background in the corresponding temperature range.

To see the anomalous peaks more clearly, we subtract the smooth background, and the results are displayed in Figs. 5 and 9, respectively for the cases I and II. We label this deviation in Heat Capacity as ΔH. The location of the peaks is at $T_{_A}^{HC} = 143.29$ K, $T_{_H}^{HC} = 314.35$ K for the case I, and in case II we find $T_{_A}^{HC} = 143.47$ K, $T_{_H}^{HC} = 310.73$ K. From the peaks at $T_{_H}^{HC}$ we find a percentage change, or deviation away from the background value, of 12.931 % and 8.125 % for cases I and II respectively. The peaks at $T_{_A}^{HC}$ represent a change of approximately 11.764 % for case I, and a 8.043 % departure from the background value, for case II.

The origin of the strong and distinct anomalous peak in the Heat Capacity at $T_{_H}$ is due to charge-orbital ordering, which supports our previous work on charge and orbital ordering using electron microscopy [6]. One can also regard this as more direct evidence for transverse and sinusoidal structural modulations. It is also tempting to suggest that this feature is related to a charge-orbital wave of e_g electrons in this material. The alteration in the manganese valence is nothing but the variation of the density of e_g electrons. The possible reason for the modulation of the manganese valence, is the successive change in the amplitude of the Jahn-Teller distortion in the MnO_6 octahedra with position [7, 8]. It is also possible to interpret the modulated structure as an orbital density wave, as mentioned previously[6]. The density of e_g electrons is constant in a pure orbital density wave, however in our case we assume that orbital state varies as shown in Fig. 6a of [6] between $\pm\pi$. It is useful to recall the description of orbital state by the pseudo-spin space[12, 13]. It is assumed that the motion of the pseudo-spin is confined to the xz plane and orbital state at the site i, $\theta_i$varies according to,

$$\theta_i \;\; = \;\; \cos(\theta_i/2)|x^2 - y^2 > + \sin(\theta_i/2)|3z^2 - r^2 > .$$

If it is assumed that a pure charge density wave, then the variation of the orbital state in the direction perpendicular to the stripe is discrete taking on values $\pm\pi$. In contrast, the Mn valence or e_g electron density varies in a sinusoidal manner. Thus it is more tempting to assume the variation of orbital-density wave to follow the variation of the charge density wave, as also proposed in [14]. In brief we take the variation of both charge density and orbital density waves to be sinusoidal. Incidentally, we can use this interpretation of the sinuosoidal variation of charge-orbital density to interpret the anomaly at $T_{_A}$. We may

simply see that in this temperature region a further alteration occurs in the charge and magnetic state of the material, perhaps involving a further change in the local structure, arising from a weak Jahn-Teller effect.

The results of the dc magnetic measurements are displayed in Figs. 10-11 for cases I and II respectively. To see the anomalous peaks more clearly, we subtract the smooth background, and the results are displayed in Figs. 11 and 13, respectively for the cases I and II. We label this deviation in Heat Capacity as ΔM. The location of the peaks is at $T_{_A}^M = 164.76$ K, and $T_{_H}^M = 323.00$ K for the case I, and in case II we find $T_{_A}^M = 164.86$ K, $T_{_H}^M = 318.73$ K. From the peaks at $T_{_H}^M$ we find a percentage change, or deviation away from the background value, of 7.69 % and 6.45 % for cases I and II respectively. The peaks at $T_{_A}^M$ represent a change of approximately 5.59 % for case I, and a 3.30 % departure from the background value, for case II.

It may be remarked that as our simulations of electron microscopy [6] are consistent with the Wigner-Crystal model, it is tempting to interpret our HC data in this context by thinking of it as signalling the formation of Wigner-Crystal at temperature $T_{_H}$. At the temperature $T_{_A}$, the anomaly may be seen to arise from the charge-orbital ordering alteration of the magnetic state of the material. The only work we located for which similar interpretation was given is [11] for the case of cobaltate polycrystalline $Pr_{0.5}Co_{0.5}$ O_3. It is interesting to note, that two anomalies have been reported for the case of the cobaltate polycrystalline $Pr_{0.5}Co_{0.5}$ O_3, [11], see Fig. 4 of [11]. The anomaly at $T_{_A}$ is attributed to the orbital-ordering alteration of the ferromagnetic state.

In order to further understand the difference between commensurate and incommensurate behavior, we present the ED diffraction pattern for case x=0.67 and x=0.60. Fig. 14 and 15 show ED patterns for x=0.67 at 80 K and 290 K respectively. Likewise, Fig. 16 and 17 show ED patterns for the case x=0.6 at 80 K and 290 K. In Fig. 16, super-lattice reflections due to charge-orbital ordering are indicated by black arrows. The hk0 reflections (h,k:odd) indicated by white arrow are the fundamental reflections of low-temperature Pccn(56) structure. The reflections are invisible in Fig. 15, indicating the structural phase transition to high-temperature Bmab(64) structure, as already mentioned. However, the super-lattice reflections due to charge-orbital ordering are still clearly visible.

In Fig. 16, the hk0 reflections are very weak. In addition, super-lattice reflections are invisible at 290K as seen in Fig. 17. From the ED experiments, it is roughly estimated that the temperature at which the super-lattice reflections appear is maximum around x=0.67. The temperature at which the hk0 reflections appear also might be maximum around x=0.67.

These observations are supported by the HC and dc magnetization studies, as indicated above. The HC and magnetization data for x=0.60 indicates that transitions are weaker as compared to x=0.67.

Low-temperature electron diffraction measurements confirmed super-lattice reflections due to the charge-orbital ordered (COO) states at doping levels of $0.55 \leq x \leq 0.75$ for $Nd_{1-x}Ca_{1+x}MnO_4$ system. High-resolution electron microscopy observations revealed transverse and sinusoidal structural distortions with a doping-level-dependent period of d_s =

$a/(1-x)$ in the COO phases. The d_s is commensurate to the lattice period at commensurate doping levels, e.g. 3a at x=0.67, or 4a at x=0.75, and incommensurate at incommensurate doping levels, e.g. 3.3a at x=0.7. The successive Jahn-Teller distortions imply successive modulations of the e_g orbital state and the Mn valence with the period of d_s. From the EM we can see, in terms of the COO states, a small but significant difference between commensurate and incommensurate doping levels. If we take the heat capacity and the dc magnetization results in addition to the EM results we can clearly see a difference between the commensurate and incommensurate dopings.

4 Conclusions

We have for the first time provided clear experimental evidence for charge-orbital ordering and related transition using Heat Capacity and dc magnetization measurements in the material $Nd_{1-x}Ca_{1+x}MnO_4$. This supports the previous HRTEM and ED experimental work of two of the authors [6], which gave evidence of the presence of a charge-orbital density wave in layered manganites $Nd_{1-x}Ca_{1+x}MnO_4$. The measurements suggest that the region near and of the anomaly is non-perturbative. In addition, we report for the first time the growth of single crystals of $Nd_{1-x}Ca_{1+x}MnO_4$, to our knowledge this has not been reported before.

Acknowledgments

The Sher Alam's work is supported by the Japan Society for for Technology [JST] through the STA fellowship and MONBUSHO via the JSPS invitation program.

References

[1] S. Alam et al.,Physica C **378-381**, (2002) 78-83.

[2] J. L. Soubeyroux et al.,J.Solid State Chemistry C **31**, (1980) 313.

[3] H. Kawanaka et al.,Physica B **329-333**, (2003) 797-798.

[4] S. Alam et al., Supercond. Sci Technol. **15**, (2002) 1330-1334.

[5] M.Imada, A.Fujimori and Y.Tokura, Rev. Mod. Phys. **70**, (1998) 1039.

[6] T. Nagai et al., Phys. Rev. **B68**, 092405 (2003).

[7] T. Nagai et al., Phys. Rev. **B65**, 060405(R) (2002).

[8] S. Larochelle et al., Phys. Rev. Lett. **87**, 095502 (2002).

[9] C.H. Chen et al., J.Appl.Phys. **81**, 4326 (1997).

[10] S. Mori et al., Nature **392**, 473 (1998).

[11] R. Mahendiran and P. Schiffer, Phys. Rev. **B68**, 024427 (2003), and references therein, in particular ref. 17.

[12] J. Kanamori, J.Appl.Phys. **31**, 14S (1960).

[13] K.I.Kugel and D.I.Khomskii, Zh. Eksp. Teor. Fiz. **64**, 1429 (1973) [Sov.Phys.JETP **37**, 725 (1973)].

[14] H. Koizumi et al., Phys. Rev. Lett. **80**, 4518 (1998).

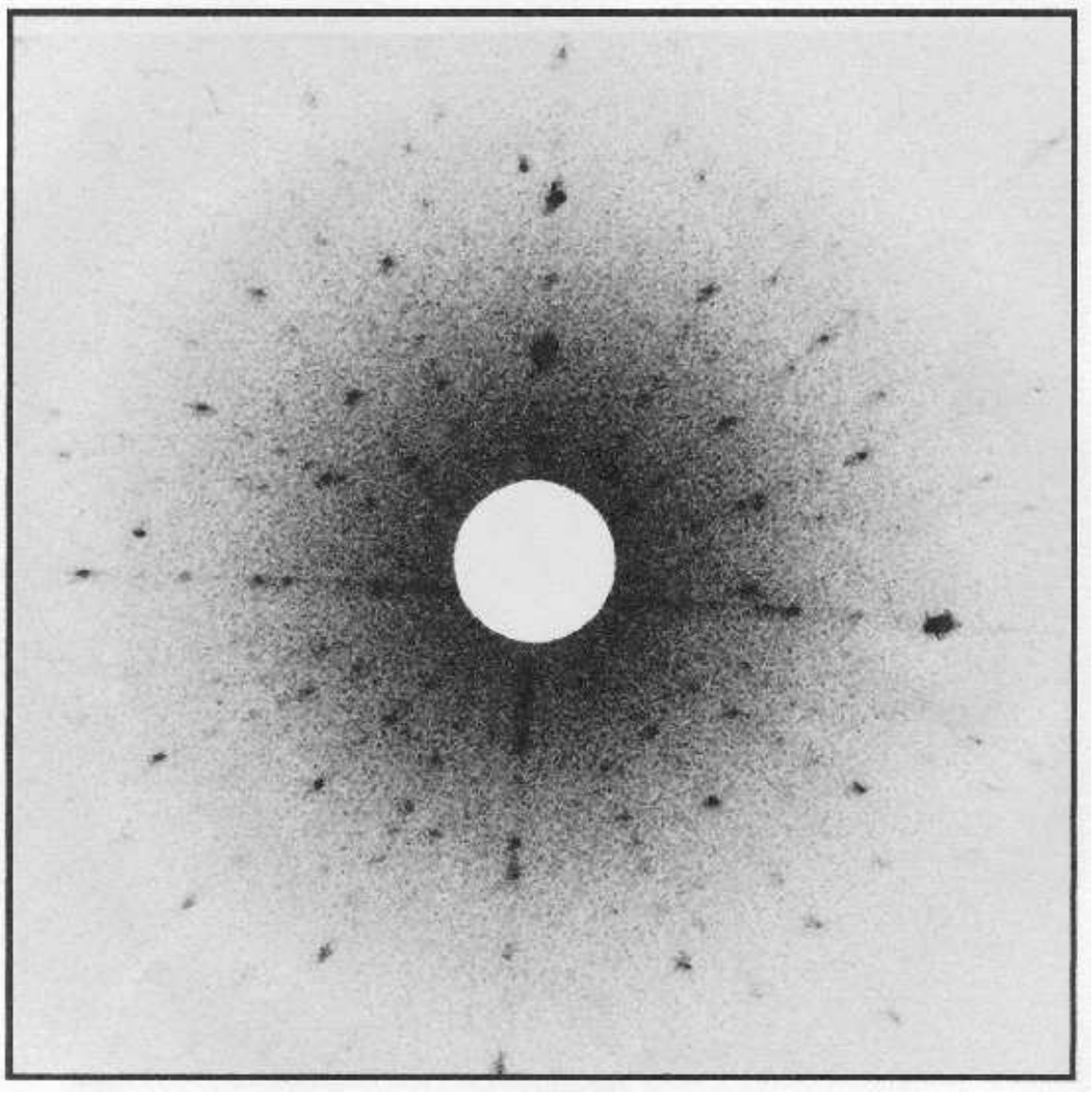

Figure 1: Laue photograph of single crystal of composition x=0.67.

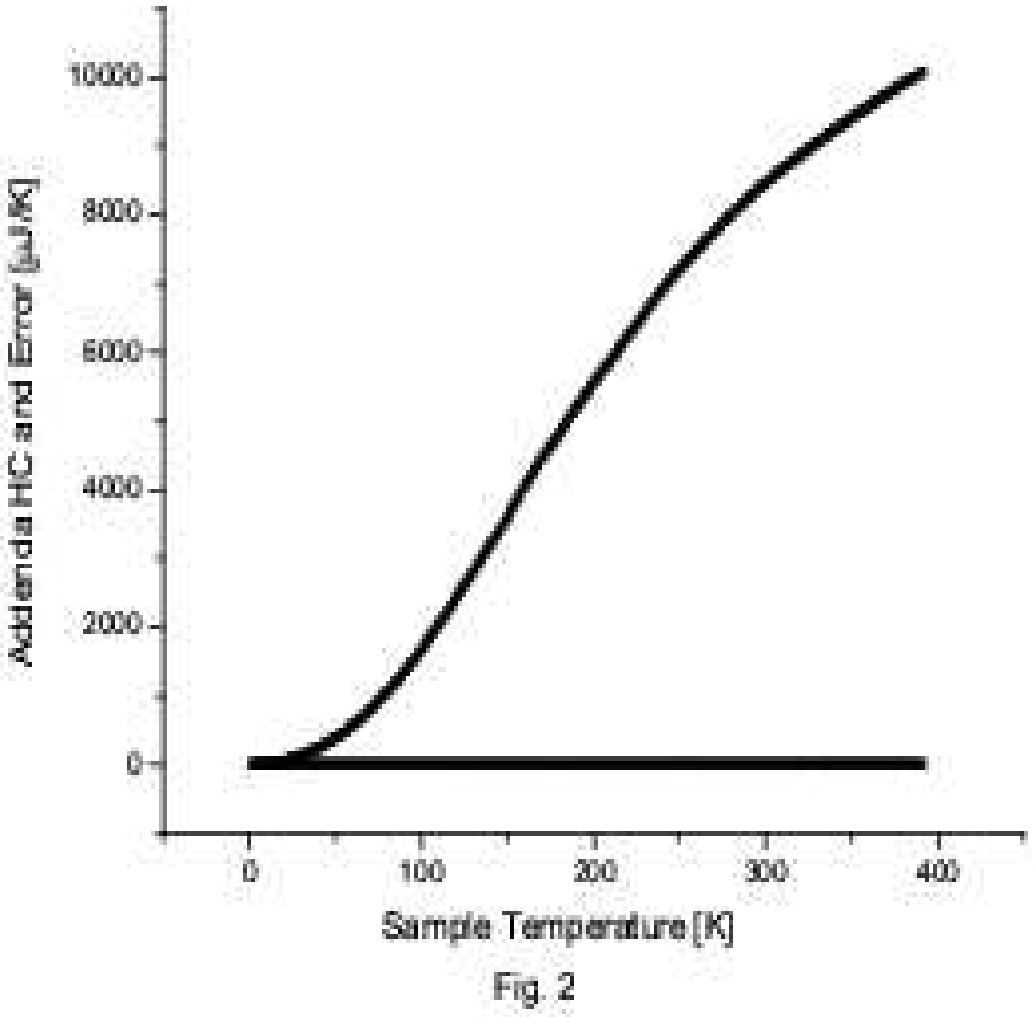

Figure 2: The Addenda HC [μ J/K] used for the $x = 0.67$ sample.

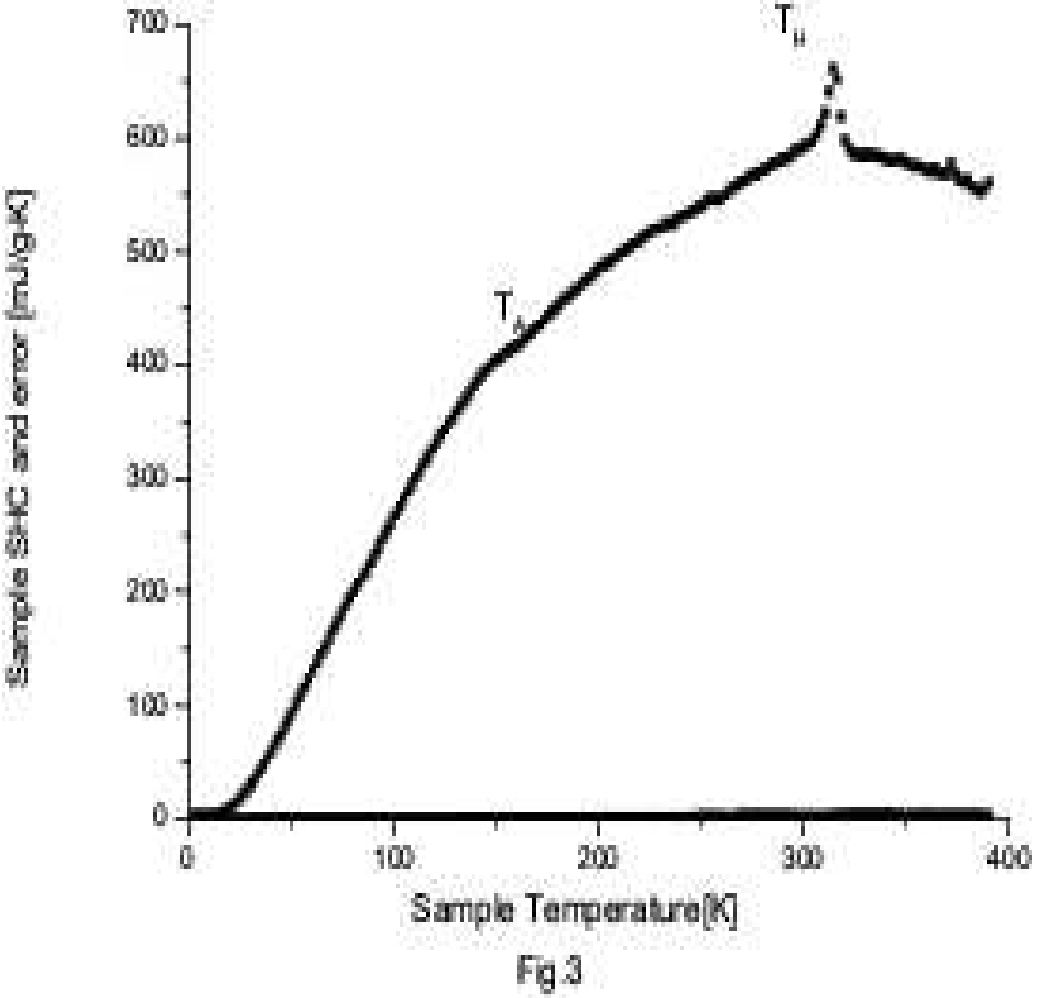

Figure 3: The sample HC and the corresponding error for the case $x = 0.67$.

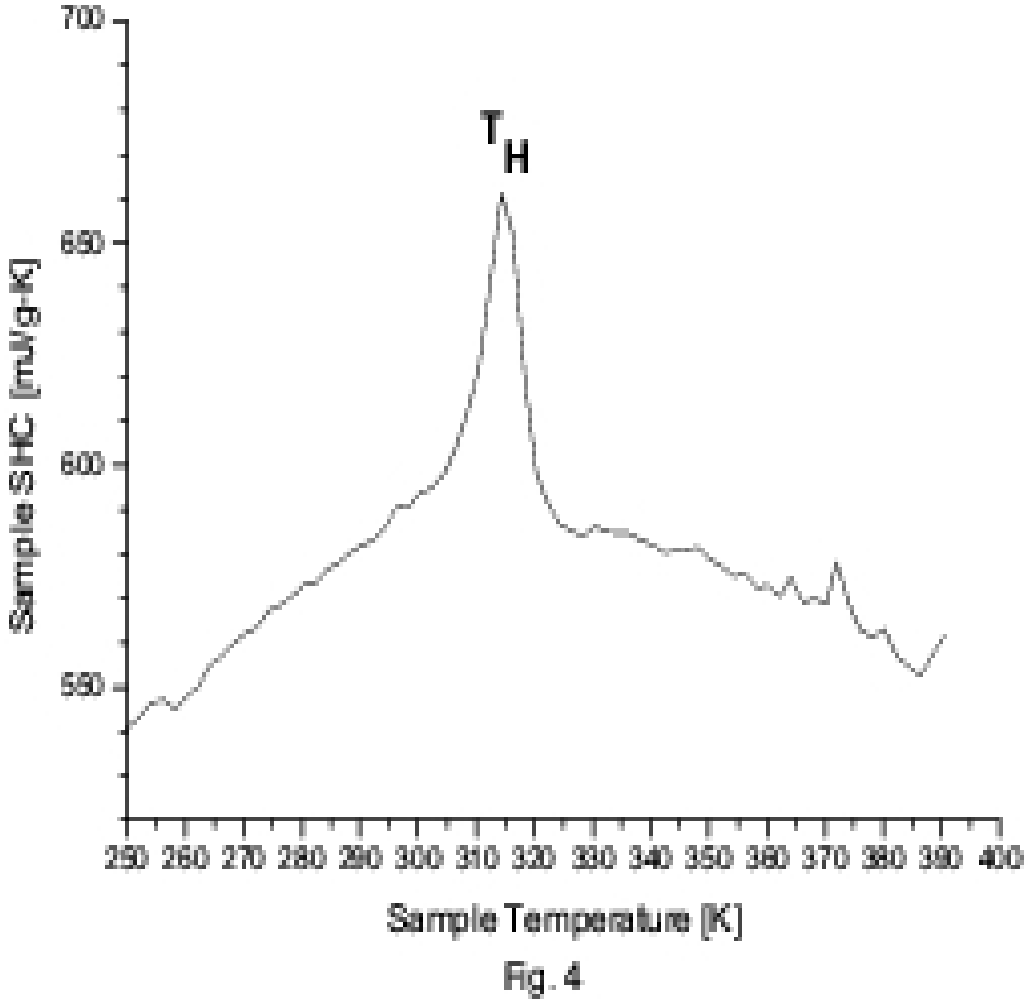

Figure 4: The main HC anomaly in more detail for the case of $x = 0.67$.

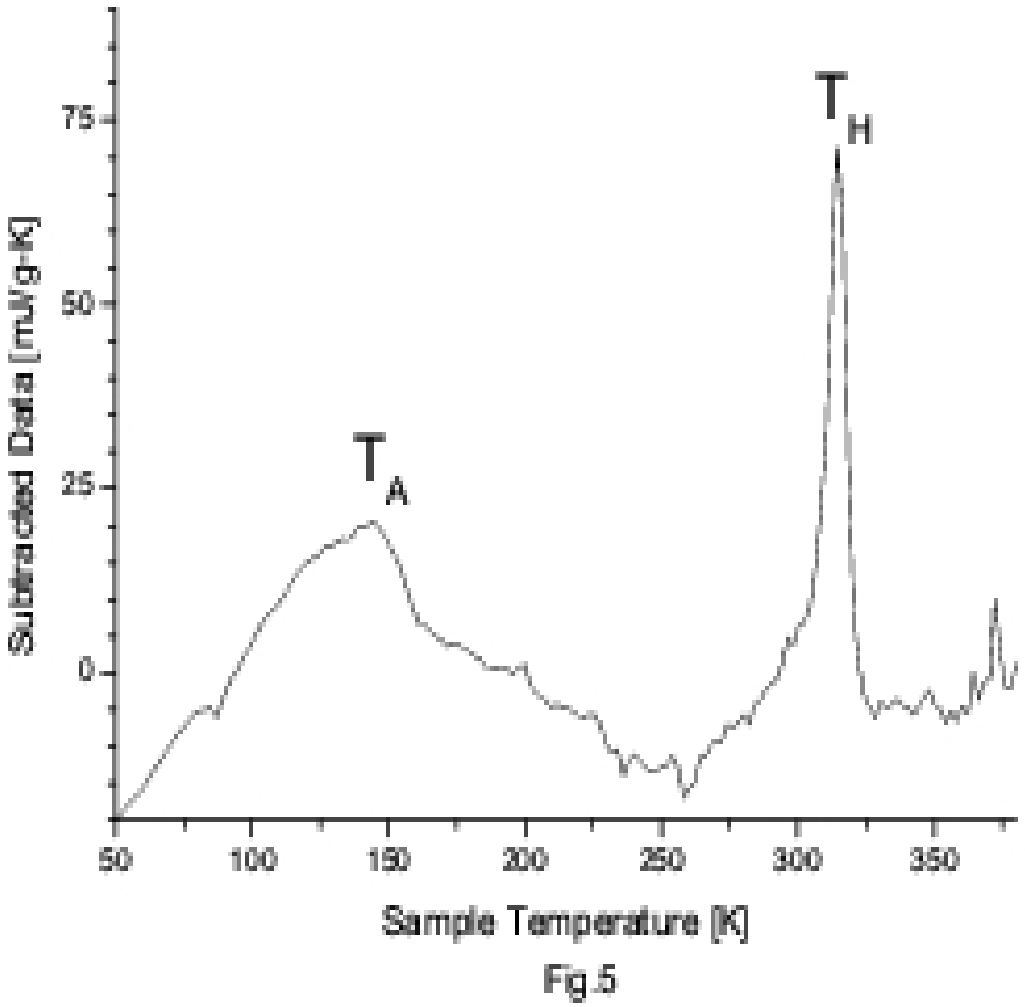

Figure 5: The subtracted data, showing the anomalies at T_H and T_A for the sample with $x = 0.67$.

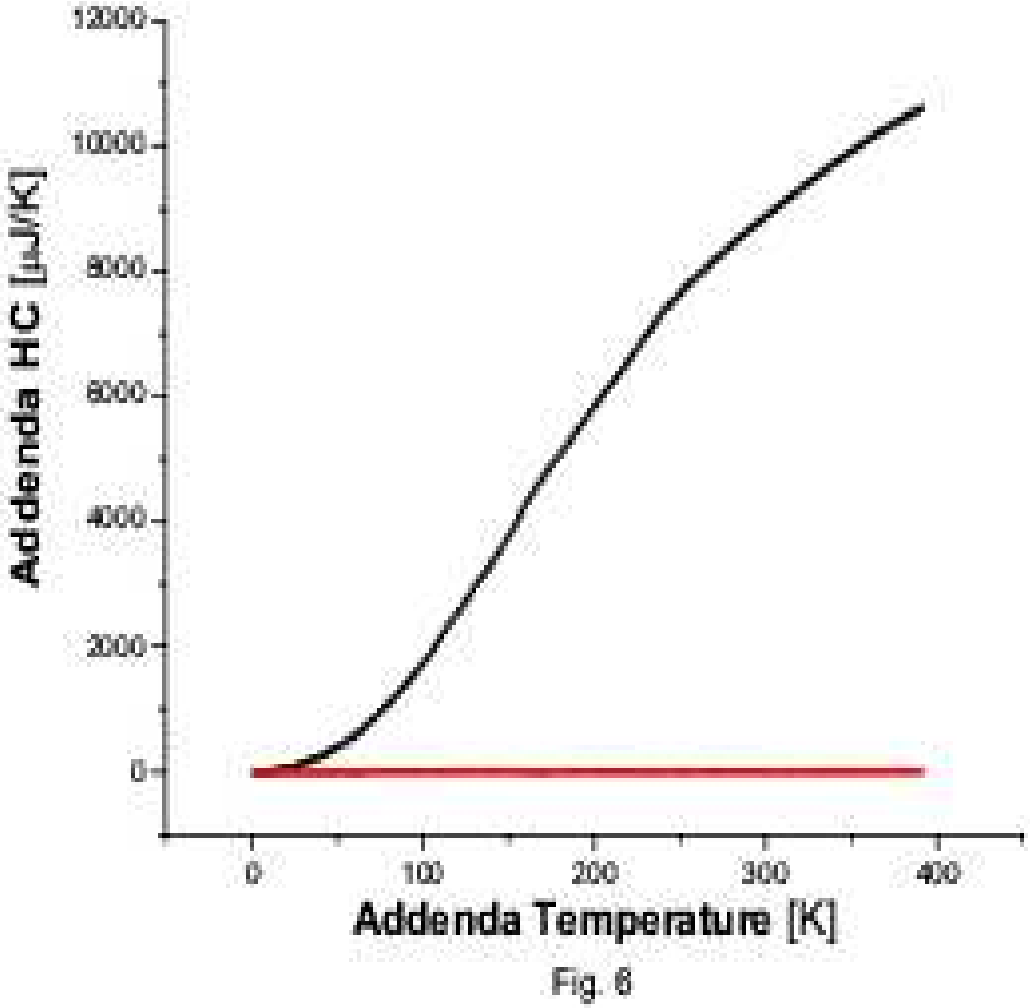

Figure 6: Results for the HC [μ J/K] of the Addenda and the error which was used for the $x = 0.70$ sample.

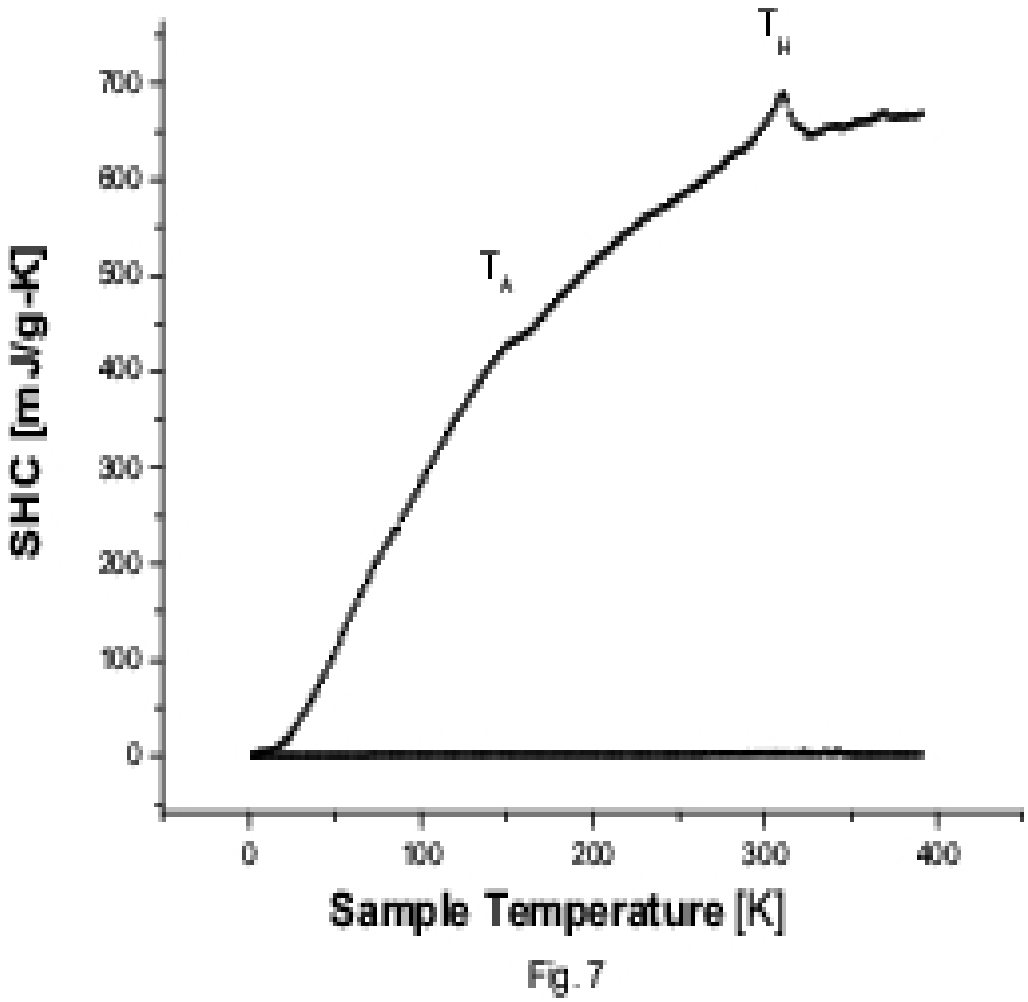

Figure 7: The sample HC and the corresponding error for the case when $x = 0.70$.

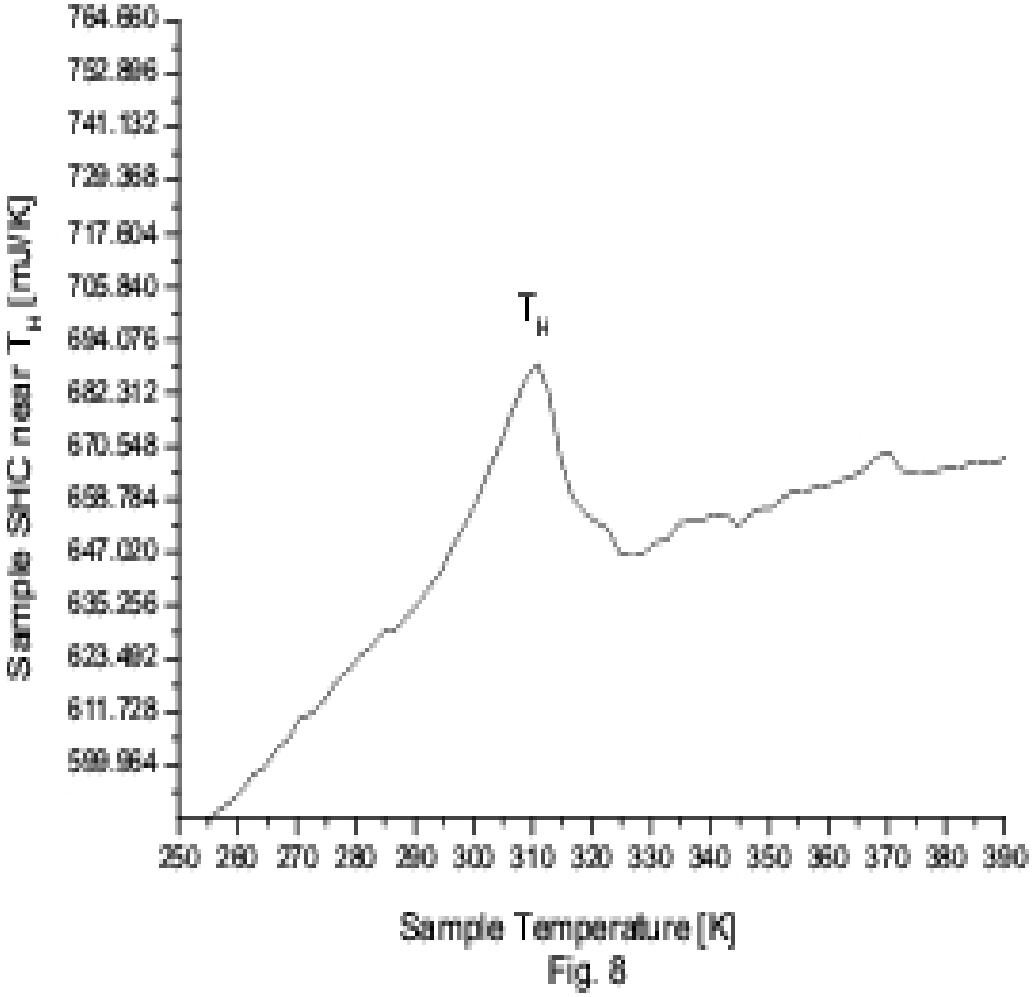

Figure 8: The main HC anomaly in more detail for the case of $x = 0.70$.

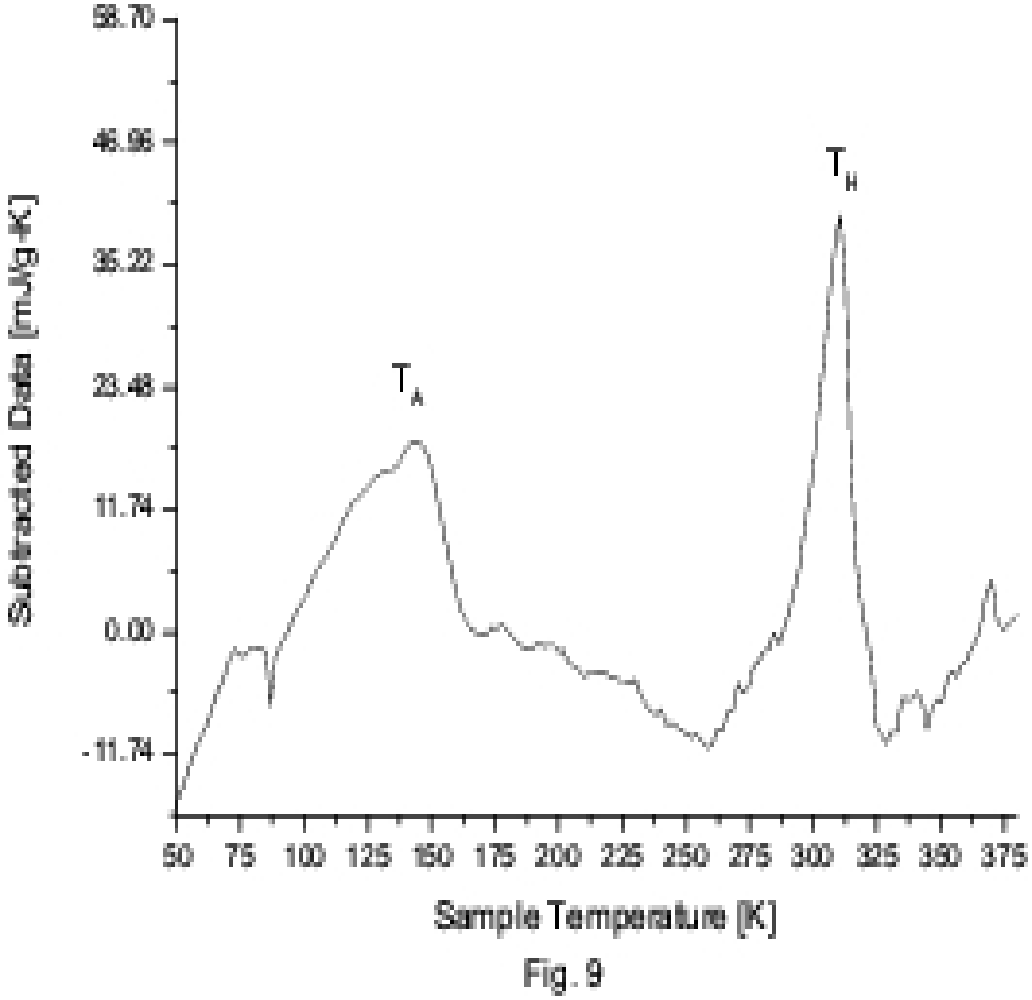

Figure 9: The subtracted data, showing the anomalies at T_H and T_A for the sample with $x = 0.70$.

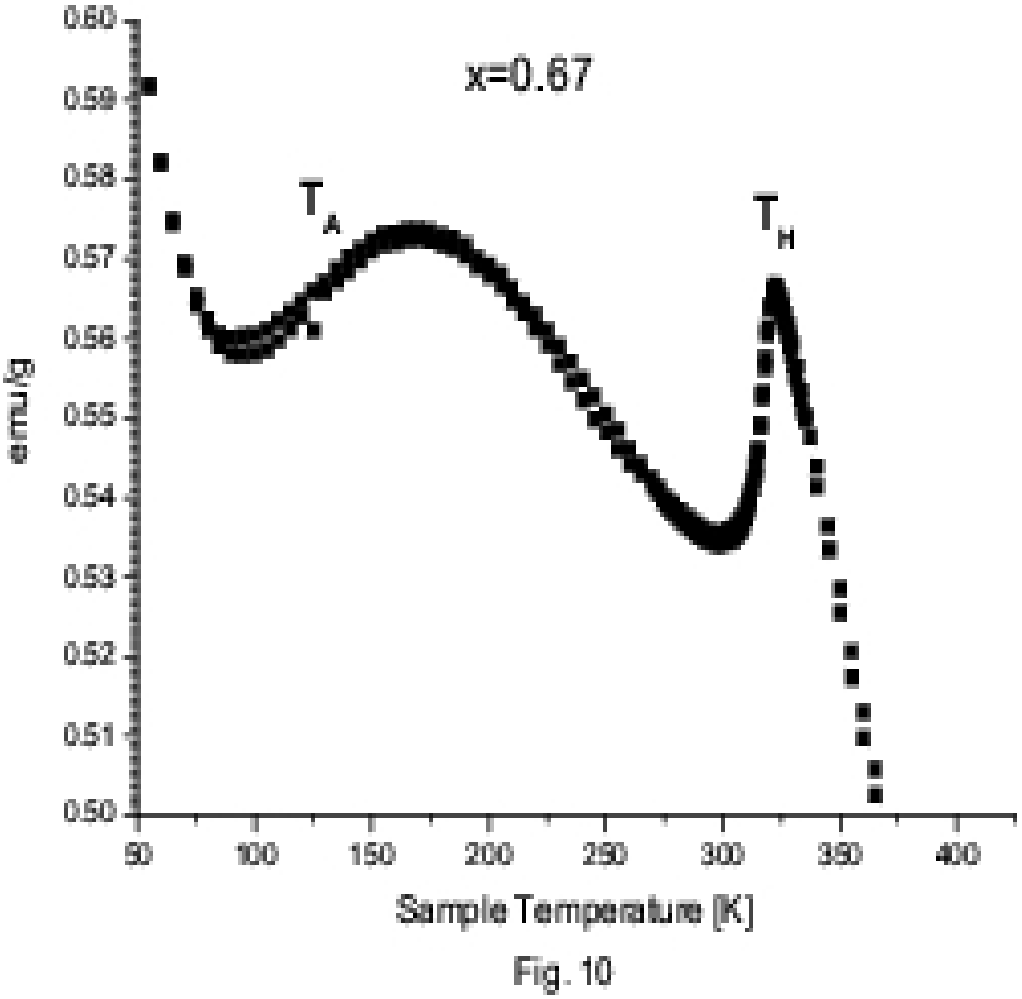

Figure 10: The Long Moment [emu/g] for the composition x=0.67, showing clearly the anomalies at T_H and T_A.The applied field is 1T.

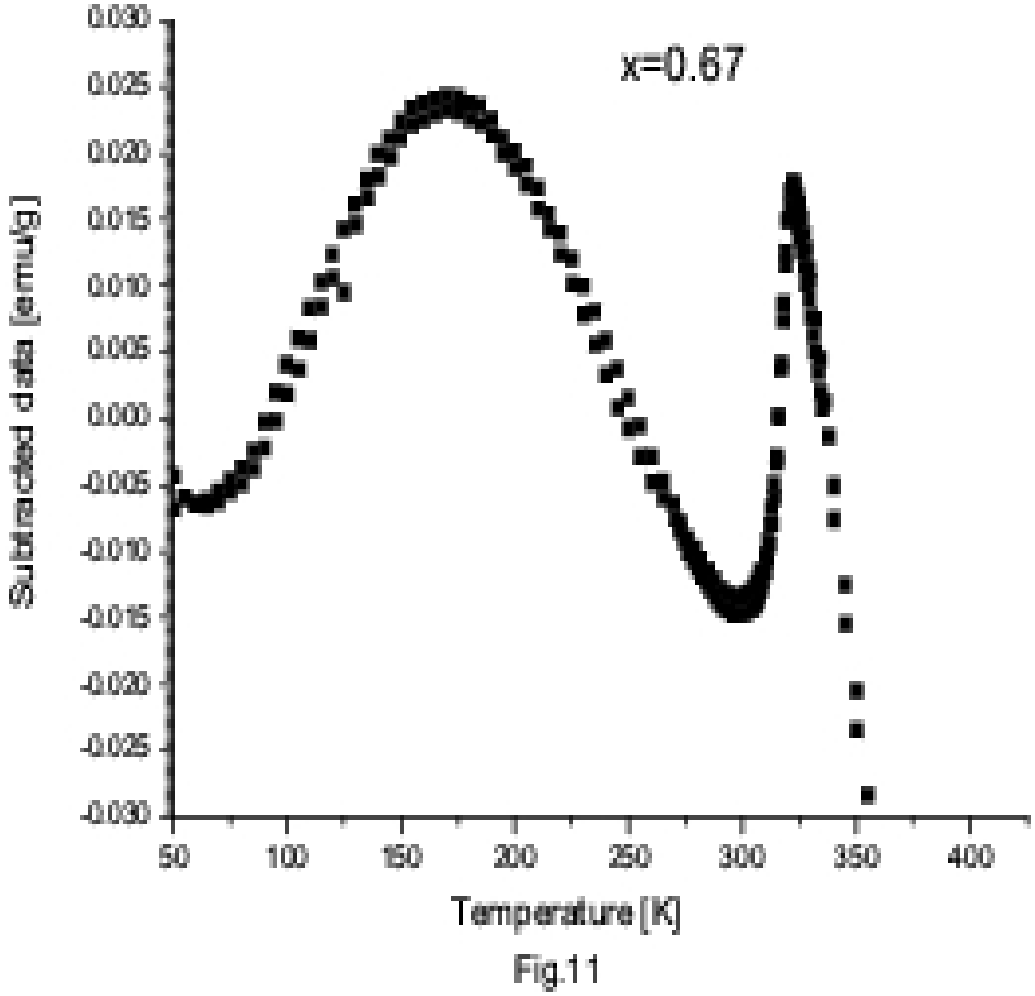

Fig.11

Figure 11: The subtracted data [emu/g] for the composition x=0.67, showing clearly the anomalies at T_H and T_A.The applied field is 1T.

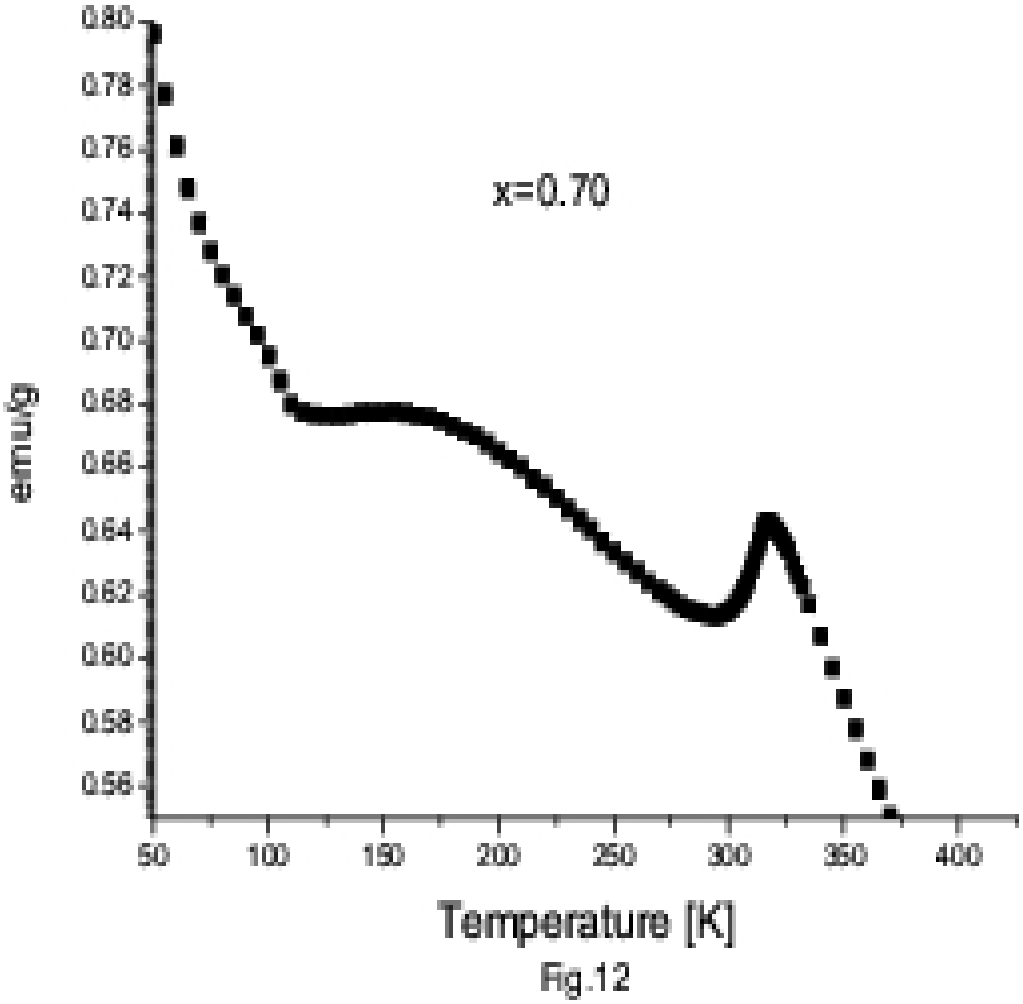

Figure 12: The Long Moment [emu/g] for the composition x=0.70, showing clearly the anomalies at T_H and T_A. The applied field is 1T.

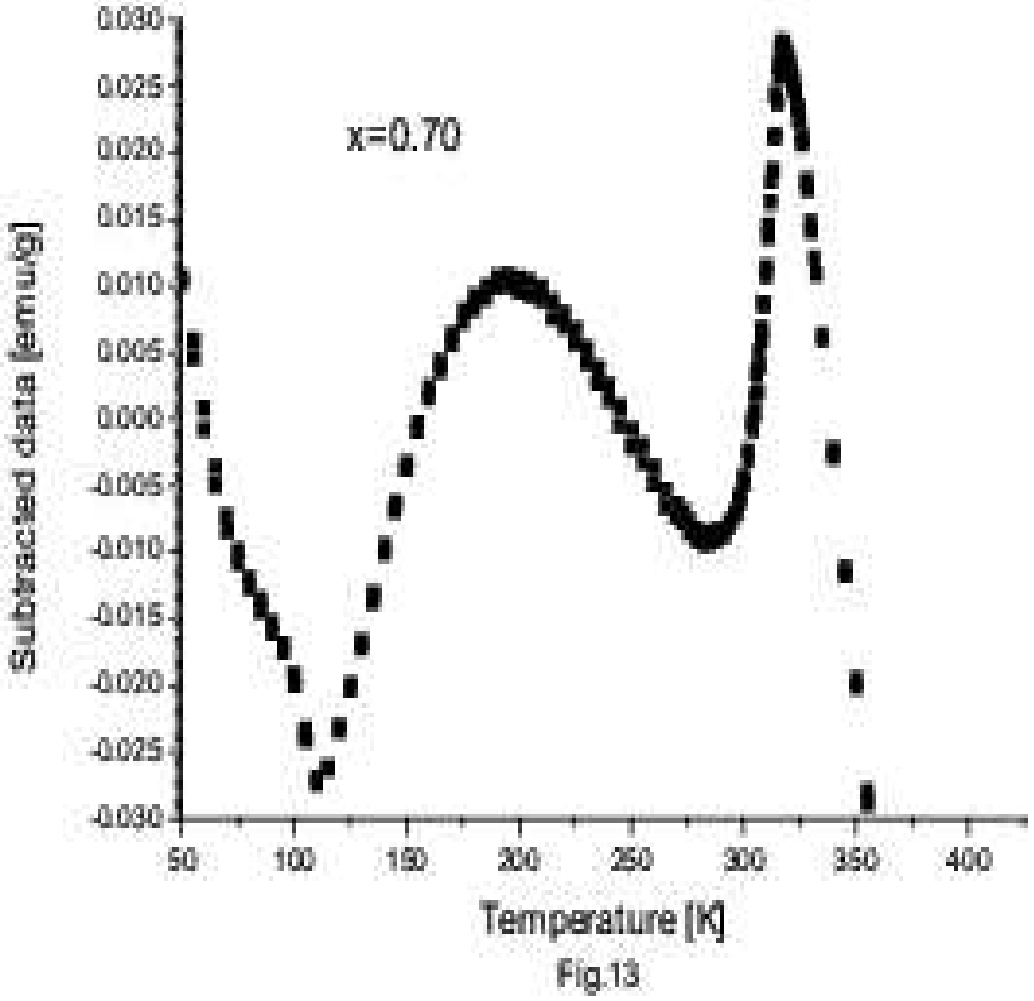

Fig.13

Figure 13: The subtracted data [emu/g] for the composition x=0.70, showing clearly the anomalies at T_H and T_A.The applied field is 1T.

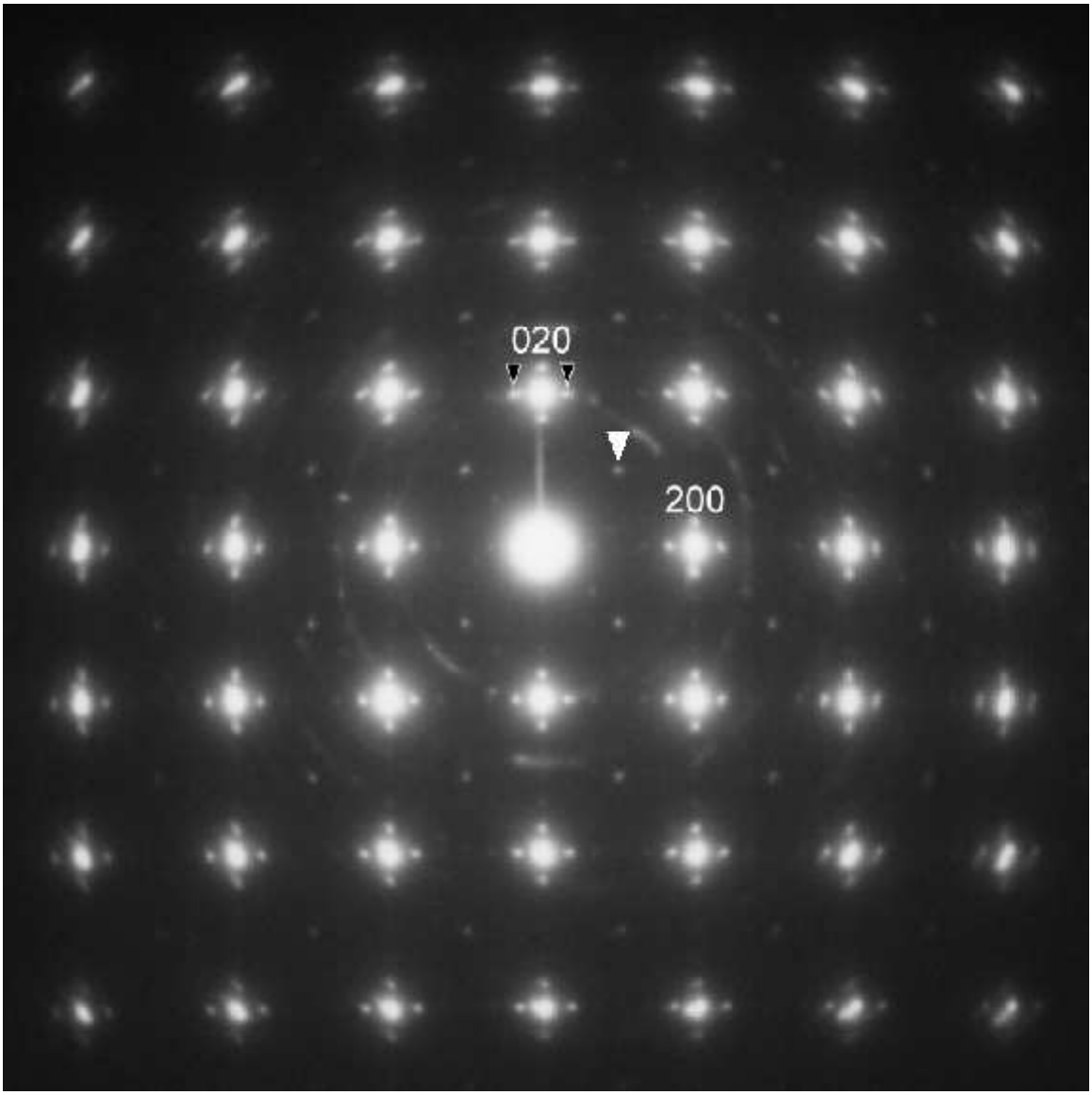

Figure 14: ED pattern for the composition x=0.67 at 80 K.

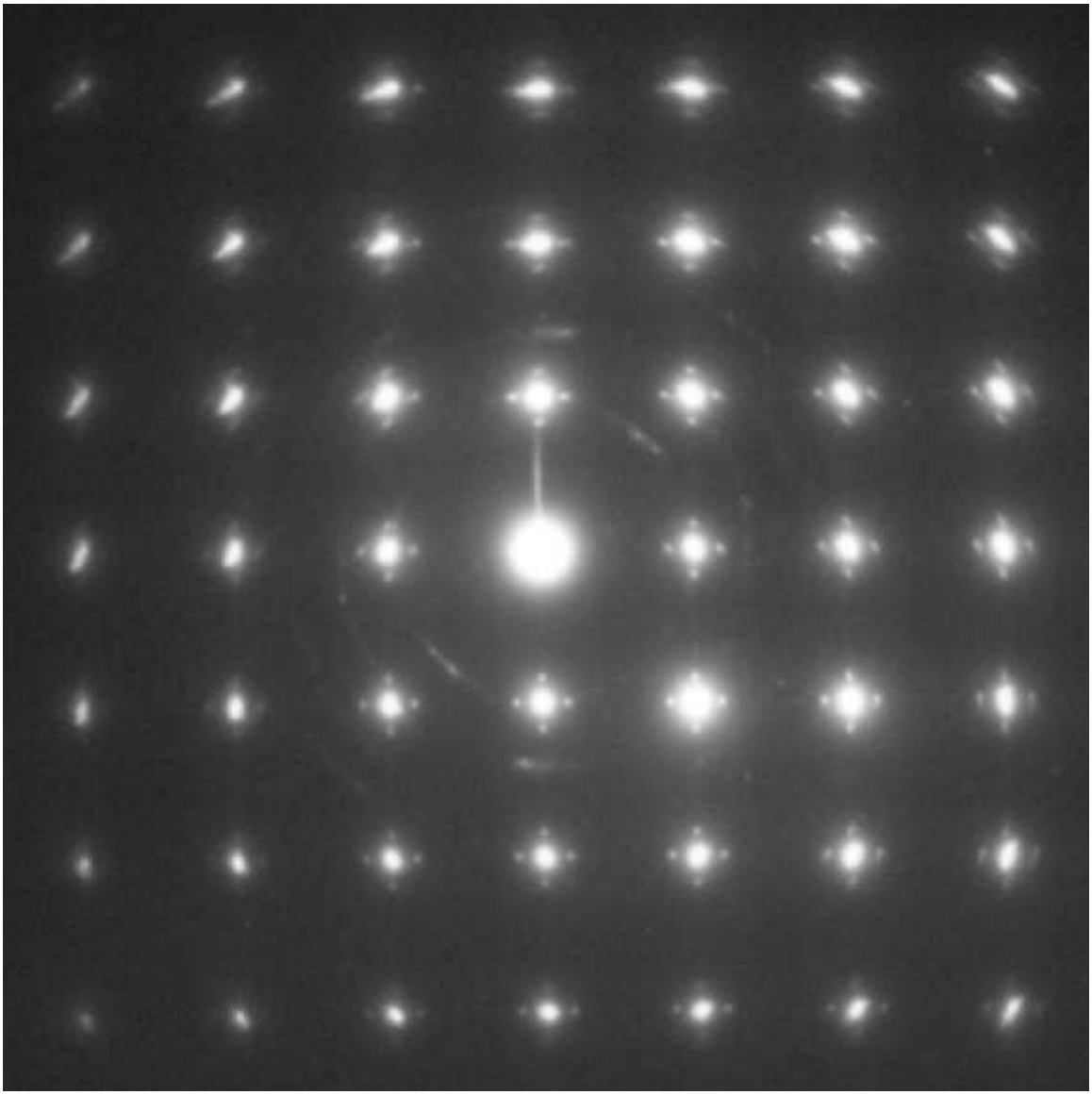

Figure 15: ED pattern for the composition x=0.67 at 290 K.

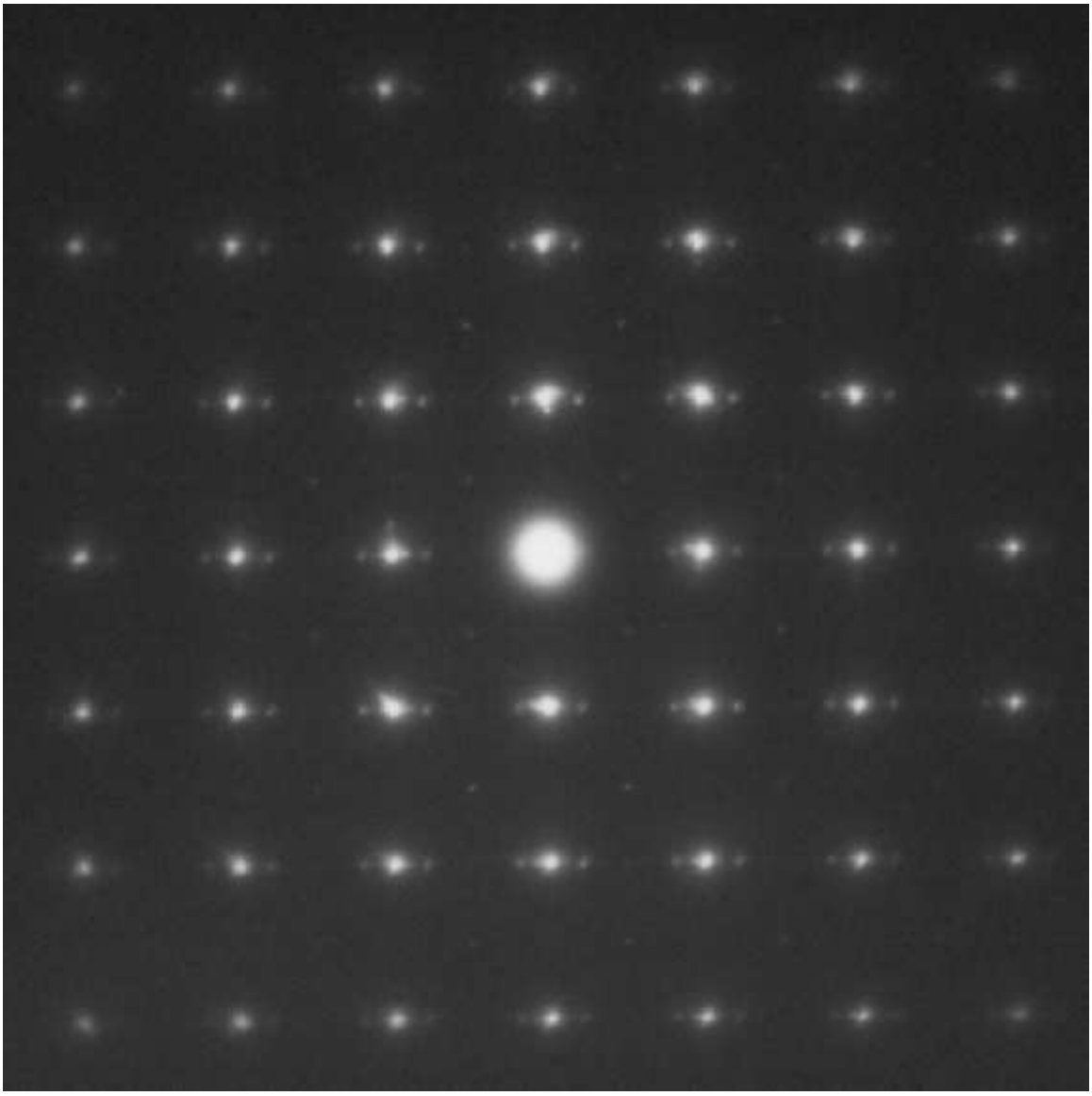

Figure 16: ED pattern for the composition x=0.60 at 80 K.

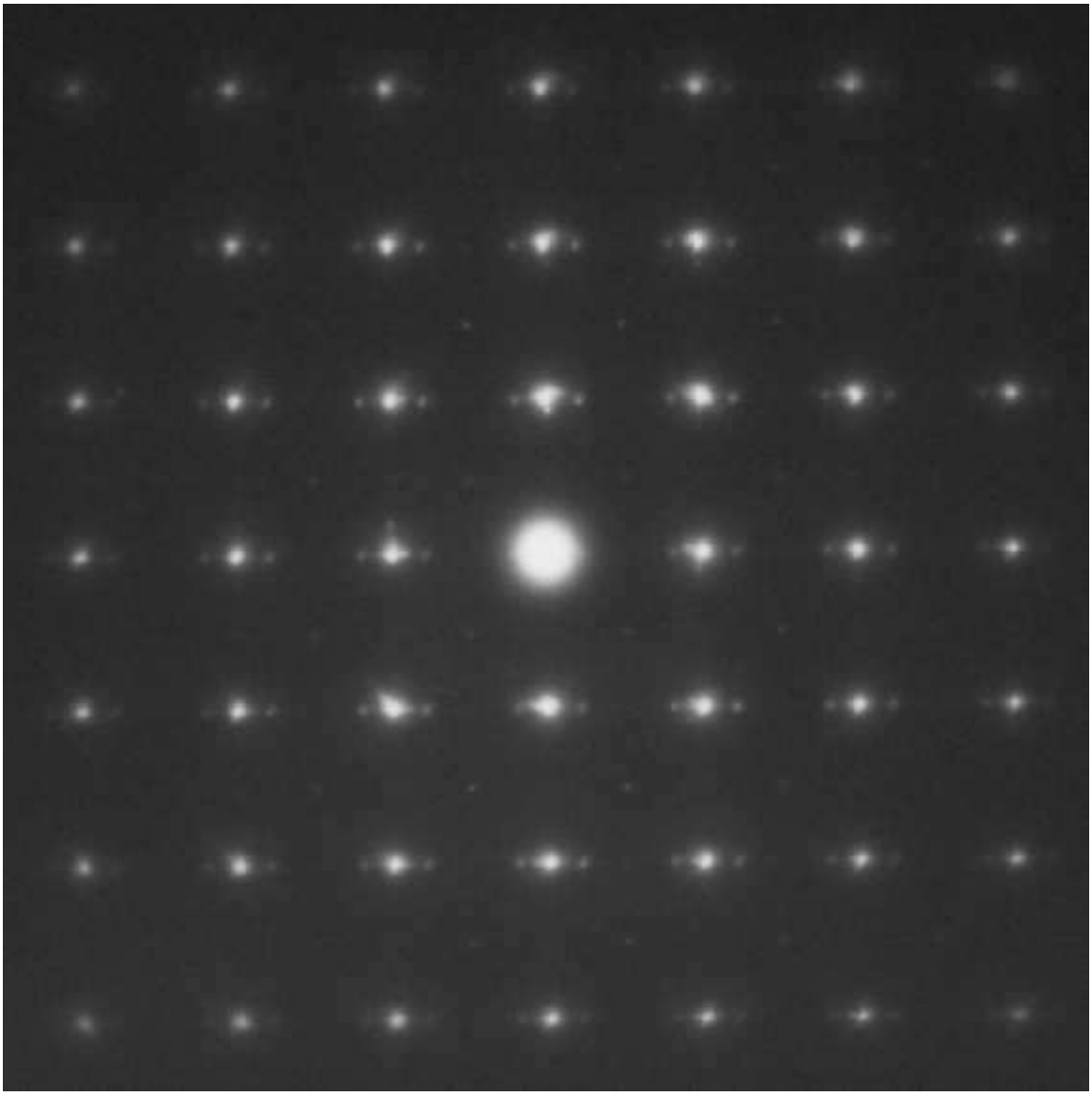

Figure 17: ED pattern for the composition x=0.60 at 290 K.